REVIEW OF THE AERONAUTICAL FATIGUE INVESTIGATIONS CONDUCTED IN POLAND WITHIN JUNE 2003 – APRIL 2005

Antoni Niepokólczycki

INSTITUTE OF AVIATION
WARSAW, POLAND

CONTENTS

INTRODUCTION

The present survey provides brief summaries of the works which have been done in Poland in the field of aeronautical fatigue during the period from June 2003 to April 2005.

The following research and industrial centres have contributed towards this survey:
- Institute of Aviation, Warsaw (ILOT),
- Warsaw University of Technology, Warsaw (PW),
- Military University of Technology, Warsaw (WAT),
- Polskie Zakłady Lotnicze in Mielec (PZL-MIELEC),
- Polskie Zakłady Lotnicze in Świdnik (PZL-ŚWIDNIK),
- Air Force Institute of Technology, Warsaw (ITWL),
- University of Technology and Agriculture, Bydgoszcz (ATR),
- Wytwórnia Sprzętu Komunikacyjnego, Kalisz (WSK-KALISZ).

The names of the people responsible for the project and their affiliations are given in brackets after the title of each item. Their full addresses are available through the author of this survey at:

Antoni Niepokólczycki
Materials & Structures Research Center
Institute of Aviation
Al. Krakowska 110/114, Warsaw, Poland
Tel. (+48-22) 846 08 01, Fax. (+48-22) 846 44 32, e-mail: antekn@ilot.edu.pl

The report aims at presenting general situation in the field of aeronautical research in Poland, especially in view of aeronautical fatigue investigations.
The recent changes, associated with the economic transformation, have strongly affected Polish aviation industry, which, as a result, became more closely integrated with international aviation industry.

Therefore two trends can be observed in the field of aeronautical investigations now:
- increased co-operation between scientific centers and industry,
- strong trends developed towards international co-operation and participation in international projects and programs.

The latter activity is clearly visible in the fields of aerodynamics and dynamics. In aeronautical fatigue investigations as a good example can serve the launching of Materials & Structures Research Center at the Institute of Aviation which resulted from the co-operation with the Pratt & Whitney Company.

The works presented have been classified into the following three groups:
- Investigations carried out by industry,
- Investigations conducted in co-operation between scientific centres and industry,
- Investigations conducted by RTD and academic centres.

The last work included in this survey *"Fatigue Loads as an Inverse Problem of the Helicopter Tail Beam Structural Dynamics"*, will be presented by one of the Authors as a poster at the 23rd ICAF Symposium in Hamburg.

INVESTIGATIONS CARRIED OUT BY INDUSTRY

Full-Scale Fatigue Testing of a Braced Wing and a Wing-Carry-Through Structure of a Commuter Aircraft – next stage of the research

(Janusz Pietruszka – PZL MIELEC)

In the previous review (Lucerne 2003) the fatigue test of a wing and a wing-load-carry-through structure of the PZL M28 "SKYTRUCK" commuter aircraft was presented.

Fig. 1. PZL M28 "SKYTRUCK"

The aircraft wings are braced, so the wing-load-carry-through structure consists of the wing struts and central part of the fuselage with the main landing gear beam. The wing structure is made from sheets and extrusions of 2024 aluminum alloy, except for the fittings which are made from steel of the grade 30HGSA.

The test has been made at the laboratory of PZL in Mielec using the MTS Aero 90-LT system supplied with 16 loading channels and 82 channels of continuous monitoring (load control channels and selected strain gauge channels).

As it was presented in the previous review the test was performed in the flight-by-flight way. After 10400 simulated flights it was observed that some bolts mounting the removable upper cover of the wing in the region of rib No. 15 were damaged. All bolts in this region were replaced by the bolts the diameter of which was increased from 4 mm to 5 mm.

After 18650 simulated flights it was observed that the stress magnitude in the forward wing spar at the rib No. 15 increased by about 10 % due to the cracks that appeared in the nose region of wing, which was treated as a structure of secondary importance.

The changes mentioned above have been introduced into the process of wing production and also applied to all the airplanes in service.

After 28878 simulated flights first drops of fuel were observed under the left outer wing.

After 31670 simulated flights a crack on bottom skin of the left outer wing was detected in the region of wing bracing fitting, fuel leakage and an increase in the stress level in the wing spar caps were observed as well. On the right outer wing a crack was also observed but there was no trace of fuel.

After 31729 simulated flights the testing process was suspended as the crack of the left outer wing increased significantly and the wing might break. The left outer wing was replaced and the testing procedure was continued.

After 36000 simulated flights a small leakage of fuel was found on the right outer wing and after 36300 simulated flights the first part of the test terminated as the crack became critical and the stress level in the wing spar caps increased significantly.

Then the critical regions of the wing were repaired:

- in the right wing in the way which is possible under exploitation conditions (Fig.2.),
- in the left wing in the way optimal from the production point of view and possible to make only in the factory.

Fig. 2. Right outer wing critical region after the repair which was made before re-starting of the fatigue test. An additional piece of skin and elongated wing bracing fitting can be seen.

After the repair the second part of the test was performed. Of course, the life time counting of new parts started from zero.

Up till now, 60000 flights (part 1 plus part 2) have been simulated, which means 60000 hours of flight.

In the second part of the test cracks were observed in structures of secondary importance. These cracks were easy to detect by inspection.

Additionally, some cracks were found in the regions which are important from the integrity of structure point of view:

- in the region of wing bracing fitting to the main landing gear beam, which is the integral element of the fuselage;
- in the rib closing the main fuel tank.

During the test the appropriate repairs were made. The life time counting of new parts started from zero.

Fatigue Analysis of an Element of the Retracted Landing Gear Actuator
(Janusz Pietruszka – PZL MIELEC)

Within the certification process of polish patrol aircraft BRYZA with the retracted landing gear there was made a fatigue test of the nose landing gear actuator according to polish military standard. PN-V-82064:2003. In the course of testing the actuator was damaged. A crack was found in the head and a small hydraulic fluid leakage was detected. The damage occurred at a cyclic pressure loading up to 150% of the nominal pressure in the aircraft system, i.e. $1.5 \cdot 15$ MPa = 22.5 MPa. The actuator lugs were free.

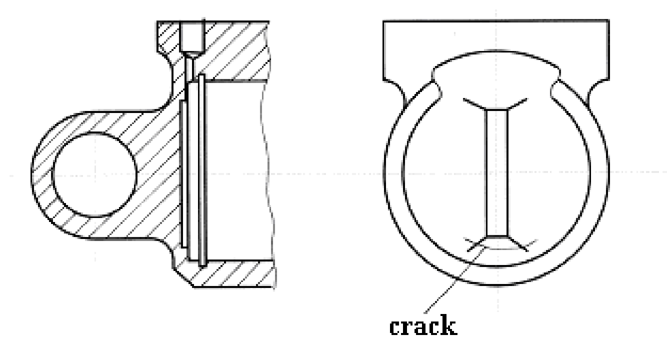

Fig. 3. Scheme of the damaged part.

The FEM calculation of the stress state were done using the MSC/NASTRAN system since the simplified calculations made before did not reveal any points of dangerous stress level.

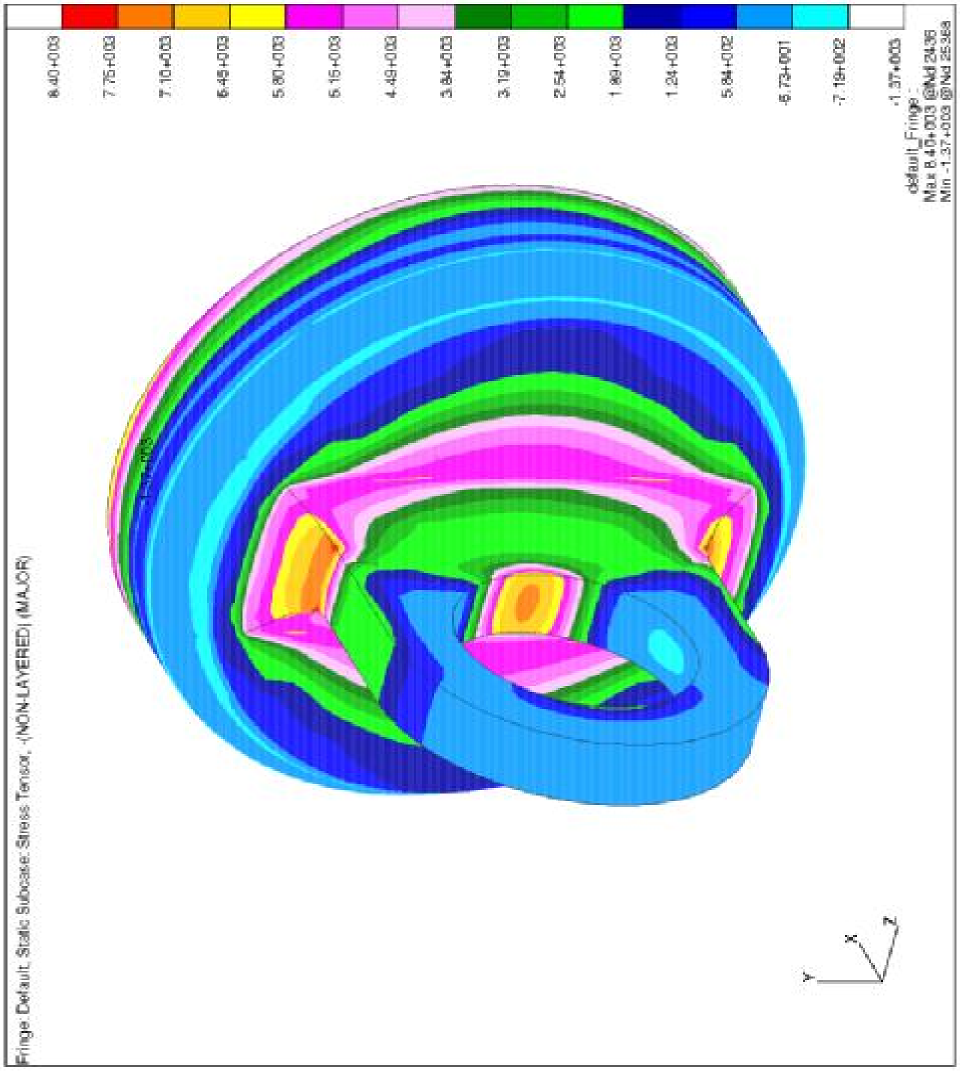

Fig. 4. The distribution of stresses over the outer surface under the loading pressure 22.5 MPa.

The calculations revealed a dangerous stress concentration in the damaged region with the maximum stress level of 840 MPa. This part is made of low alloy chromium-manganese-silicium 30HGSA steel quenched and tempered to Ftu = 1000÷1200MPa. For the maximum operating load of the actuator a significantly lower stress level resulted from calculations.

The FEM analysis results proved that blinding of the small hole was reasonable.

Comparative Fatigue Tests of Aluminum Alloy Skin Samples
(Janusz Pietruszka – PZL MIELEC)

Comparative fatigue tests of skin sheet samples made of aluminum alloys D16CzATV and of 2024-T3 clad, respectively, were performed as part of the activity in the field of replacing the Russian aluminum alloy skin sheet with a Polish material. The shape of specimens, shown in the figure below, represents typical regions of fittings and other part mountings to the wing structure.

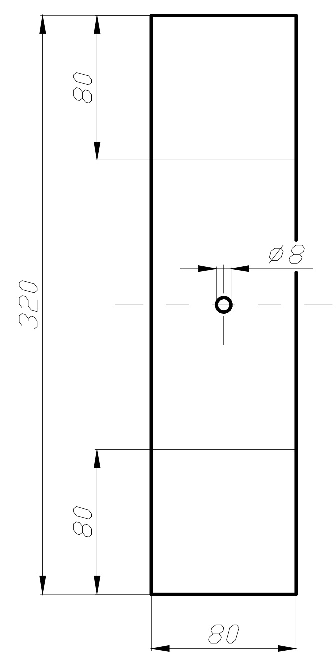

Fig.5. Geometry of the specimen used in comparative fatigue tests of aluminum alloy skin sheet; i.e., dimensions 320 mm x 80 mm, thickness 1.2mm. Each specimen has an initial hole of diameter 8 mm, which is then enlarged

The tests were made in the laboratory of PZL Mielec using the 1255 INSTRON test machine. In the test program there were preset 4 load levels of the stress ratio $R \approx 0$ at the test frequency range from 20 to 25 Hz for the purposes of testing of the fatigue life within the range from 10^4 to 10^6. At one test level there were 8 specimens of both materials.

From the tests, which have been made up till now it occurred that similar results were obtained for both the materials (see Table 1).

	Grade D16czATV	Grade: 2024-T3 clad
Stress magnitude in the critical section (without the stress contraction factor) (σmin ÷ σmax)	6 MPa ÷ 144 MPa	
Ultimate strength (Rm)	458 MPa	457 MPa
Mean logN	4.8356	4.9187
Standard deviation of logN	0.0298	0.0316
Mean N	68482	82927

Table 1. Specimen ultimate strength measurement results and the number of cycles-to-failure at a sample load level.

The testing process is in progress now. The results obtained up till now have proved that it is possible to replace the skin sheet of D16czATW with 2024-T3 clad from the given supplier.

Fatigue Test of the Wing Flap Control System Lever
(Janusz Pietruszka – PZL MIELEC)

Within the certification process of the wing flap control system levers after the lever material has been changed, i.e. it is made of Polish magnesium cast alloy GA-8 (according to polish standard) a fatigue test was performed on the lever part revealing the highest stress level. Since the lever arms make an acute angle a stress concentration may emerge in that region. The test program was very simple, because high loads are acting upon the lever during the take-off and approach to landing, which gives two load pulses per one flight. The lever was mounted to the rig as in the aircraft – see photo below. To one lever end a force was applied and the other one was clamped. The test was performed in blocs, i.e. after each 3000 cycles the load parameters were changed, since during the take-off (flaps extended to the angle of 15^{o}) and landing (flaps extended to the angle of 40^{o}) different forces are acting upon the lever in different directions. During the test a strain gauge measurements were made to verify the theoretical values and to observe possible damages in a better way.

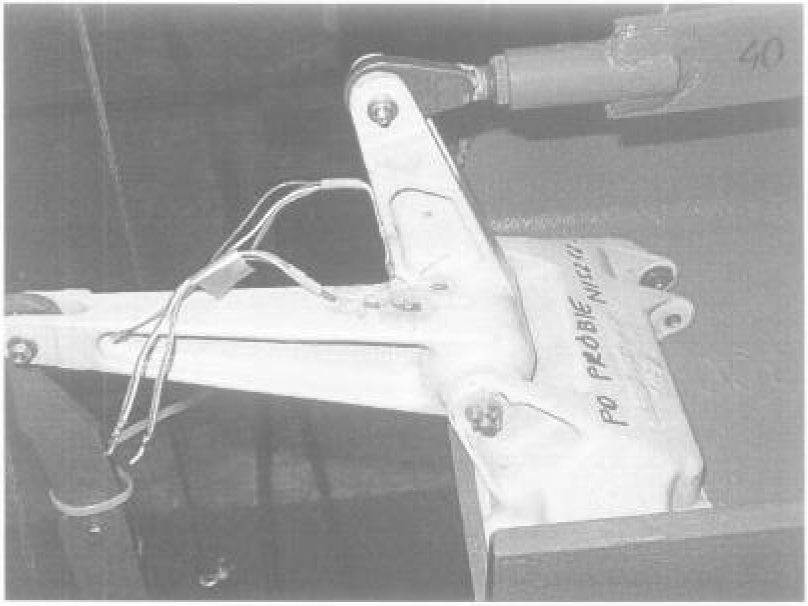

Fig.6. The wing flap control system lever

After 48 000 simulated flights a crack was observed at the expected point, although the indications of strain gauges remained unchanged (maximum stress level was 87 MPa with Ftu min = 183 MPa).

The test was then continued. After performing 60000 flights the strain gauge indications began to change due to the crack propagation. After 114000 flights the test was terminated, because the lever was permanently damaged due to a large crack.

The following lever service life resulted from the test:

114 000 / 5 = 22 800 flights

where 5 – the assumed scatter of test results.

Certification Program of the PZL SW-4 Helicopter

(Wiesław Kanadys – PZL Swidnik)

<u>Introduction</u>

In accordance with the requirements of JAR 27.571(a) and ACJ 27X602 as well as the CRITICAL PARTS PLAN standing in PZL-Świdnik, the FFMEA (Functional Failure and Effect Analysis) was carried out for all structural sections of the SW-4 helicopter.

The analysis results allowed for a choice of the critical parts, the failure of which during operation on ground or in flight may lead to the rotorcraft crash.

These parts were classified into 3 categories.

The parts of class A are subject to fatigue loads and reveal the life times shorter than the aircraft service life. There are 115 such parts made in PZL Świdnik and 4 such parts made elsewhere (a tension member made by LORD, the blade vibration absorber from PZL Hydral, a hydraulic actuator made by GOODRICH and the Rolls-Royce engine).

The parts of class B are subject to static loads and reveal a relatively low strength margin. Parts of this class are not installed in the PZL SW-4 helicopter.

The parts of class C are either those subject to fatigue loads with life times longer than the aircraft service life, or subject to static loads with a high strength margin or the parts other than those mentioned above. There are 141 such items in the helicopter.

The above numbers do not include the main gearbox and the tail gearbox for which the manufacturer, i.e. PZL-Rzeszów does not implement the critical part classification. Both gearboxes comprise 47 critical parts.

All 307 critical parts are given in the List of Critical Parts in PZL SW-4 Product (SW-60-077).

Procedure

The "SAFE-LIFE" method was used for all the structural parts to determine the safe fatigue life of each part. The method for the fatigue life determination is based on the hypothesis of linear accumulation of fatigue damages, using the results of fatigue tests made on specimens of the real structure constructed on 1:1 scale.

The fatigue tests were performed for separate helicopter assemblies such as hubs, main rotor and tail rotor blades, control system, gearboxes, control surfaces, landing gear, etc.
Some tests were made on sections of the helicopter fuselage.
The tests of complex assemblies were usually divided into the tests of smaller subassemblies.
For example, the main rotor hub tests comprised the following 5 tests:
- test of the head in the plane of thrust,
- test of the hub arm in the plane of rotation,
- test of the blade pitch,
- test of feathering pitch hinge with the main rotor blade root (tested together),
- test of the tension-torsion strap together with the insert.

In fatigue tests the loads were increased as compared to the corresponding ones from the flying condition spectrum by about 3 times, minimum 2 times.

In tests of the assemblies for which the Ground-Air-Ground (GAG) cycles are crucial, the stresses were multiplied by a factor of 1 to 1.2 while the number of cycles – by the factor of 10. The number of cycles in the test was increased as compared to the expected number of GAG cycles during the exploitation.

The loads were determined using the results of in-flight measurements made under extreme operation conditions and allowing for the expected operation spectrum.

Analysis of the tests results

The software developed in PZL-Świdnik was employed in analysis of the fatigue test results and for determination the fatigue life of parts.

The analysis was carried out for all the critical parts subject to fatigue loads as well as for some non-critical parts the failure of which would not cause a crash but could limit the airworthiness (for example: fan shaft, horizontal stabilizer or fin).

The figure presents the identified critical areas of the pitch (feather) hinge (holes for the blade attachment bolts).

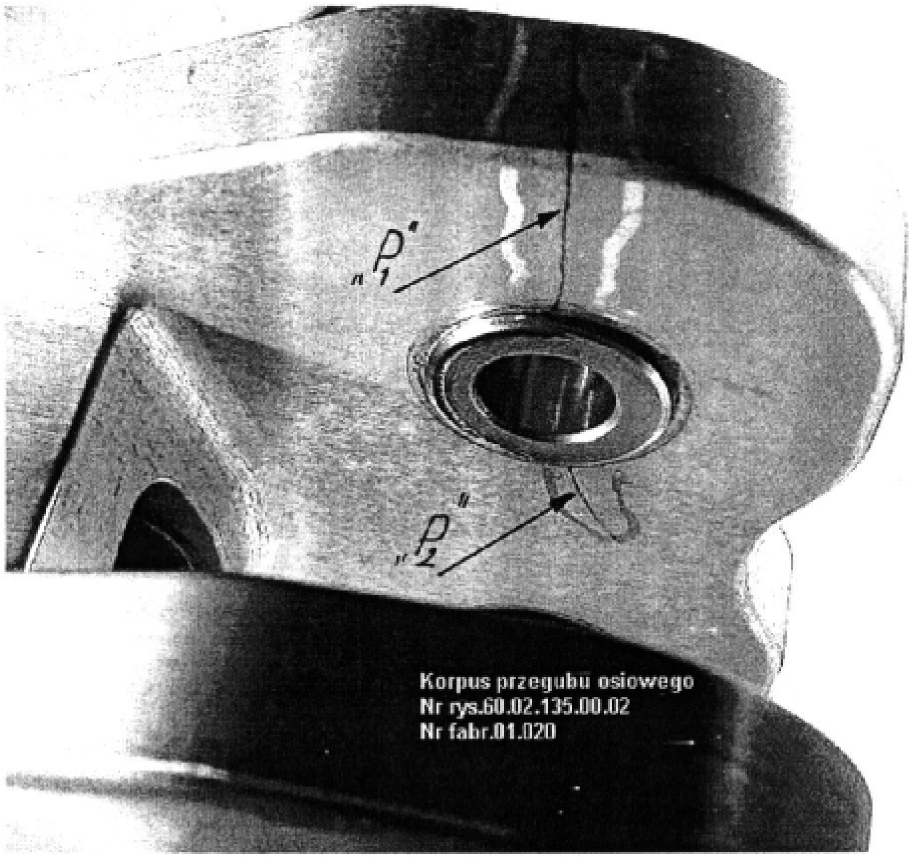

Fig. 7. The identified critical areas of the pitch (feather) hinge

The results for every specimen are processed statistically:
the average value, the standard deflection and the minimum value are determined, and then the guaranteed fatigue curve for a given critical part is determined in terms of dividing the worst test result by the stress-induced safety factor.

The value of safety factor is determined taking the number of tested specimens, number of measurements in flight and scatter of test results into account as well as the acceptable probability of damage of a particular element which depends on its level of importance.
The allowable damage probability for critical parts is 0.001, while for the non-critical ones is 0.01.

Besides the aforementioned stress-dependent safety factor additional safety factors are used depending on the number of cycles and taking the following issues into account:

- difference between the load frequencies in test and in flight,
- lack of low-cycles in test,
- error due to application of the linear damage accumulation hypothesis.

The total value of safety factor versus the number of cycles is from 1 to 8 (most often 2).

As a result the fatigue curves for particular specimens and the guaranteed curve were obtained.

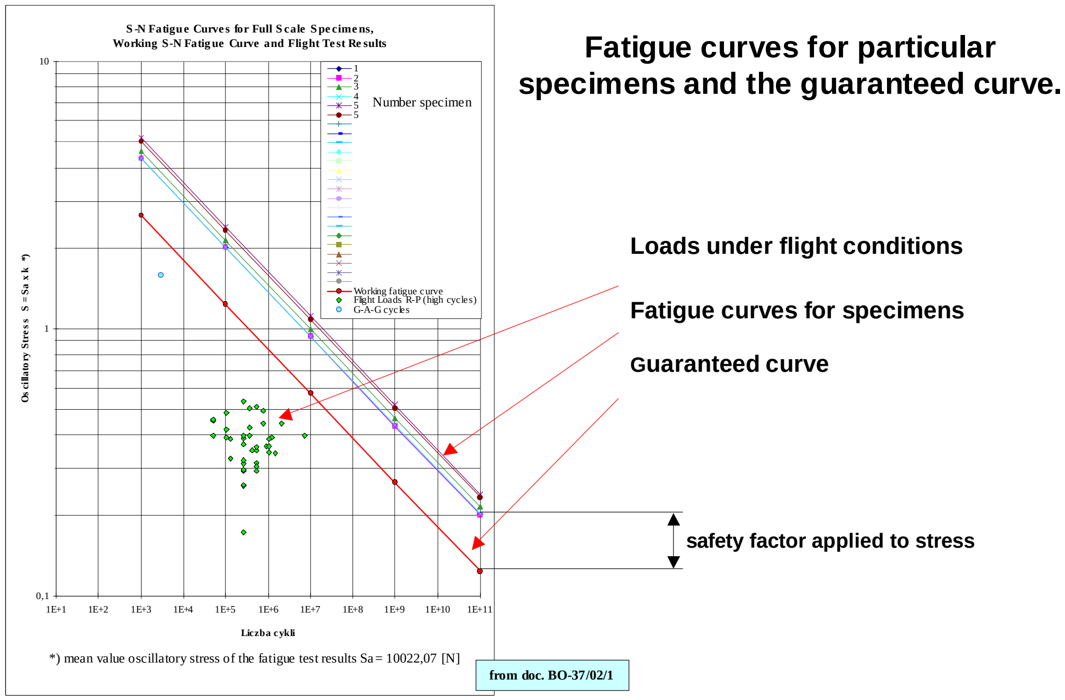

Fig. 8.

INVESTIGATIONS CONDUCTED IN CO-OPERATION BETWEEN SCIENTIFIC CENTERS AND INDUSTRY

Primary Analysis of the Causes of Crack Initiation in the Asz-62IR Aircraft Engine Crankcase

(Mieczysław Bengier – WSK KALISZ, Wiesław Ostapski – PW)
(in co-operation with WAT)

The aircraft piston engine type Asz-62IR (Fig. 9.) is a single row nine cylinder, air-cooled engine with the reduction gear. It is used in the AN-2 and M-18 aircraft. The engine is very reliable in operation under extremely difficult weather conditions; e.g., in arctic and desert climates.

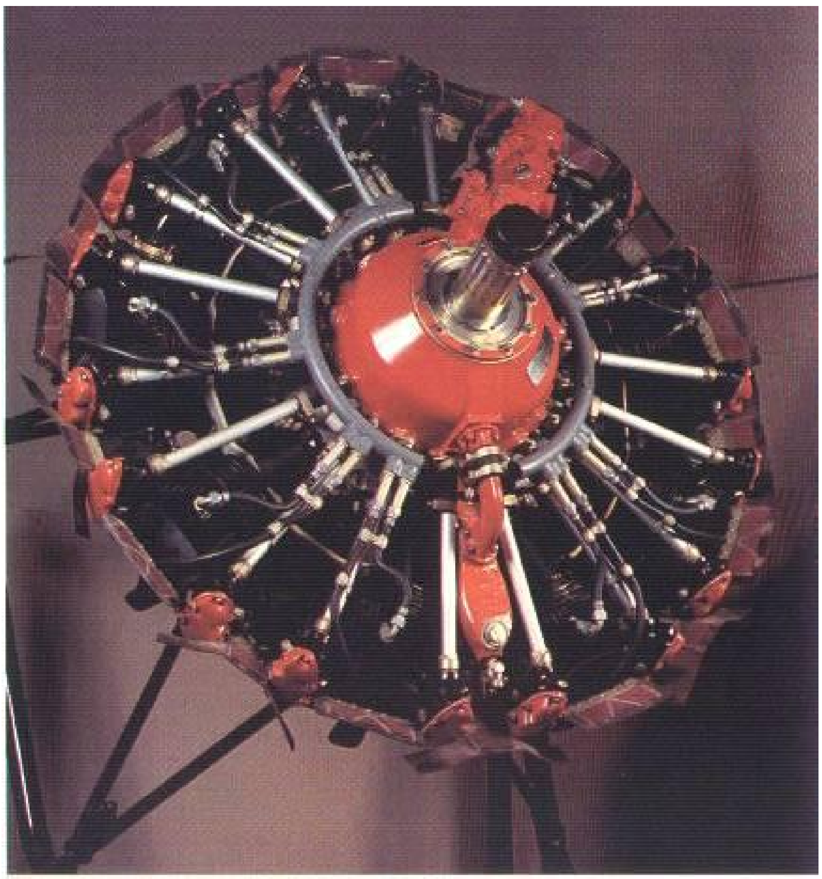

Fig. 9. Aircraft piston engine of the type Asz-62IR

The ASz-62IR engine meets the requirements of FAR-33 and has met the certification requirements of Poland, Canada, Brazil, China and the USA.

The factory is proud of the outstanding quality of all of its products, especially of the fact that there has never been a plane lost due to the failure of an engine manufactured by WSK Kalisz.

One of the most important tasks realized by WSK KALISZ is a continuous monitoring of its engines being in service. During the inspections of ASz-62IR engines which were used in agricultural and fire-fighting aircraft, the cracks crankcases were observed in the crankcases(Fig. 10.). The cracks were analyzed in view of following five aspects:

- structure of the crankcases,
- number of cracks,
- area of the crack appearance,
- time of crack nucleation,
- crack propagation (growth rate and direction).

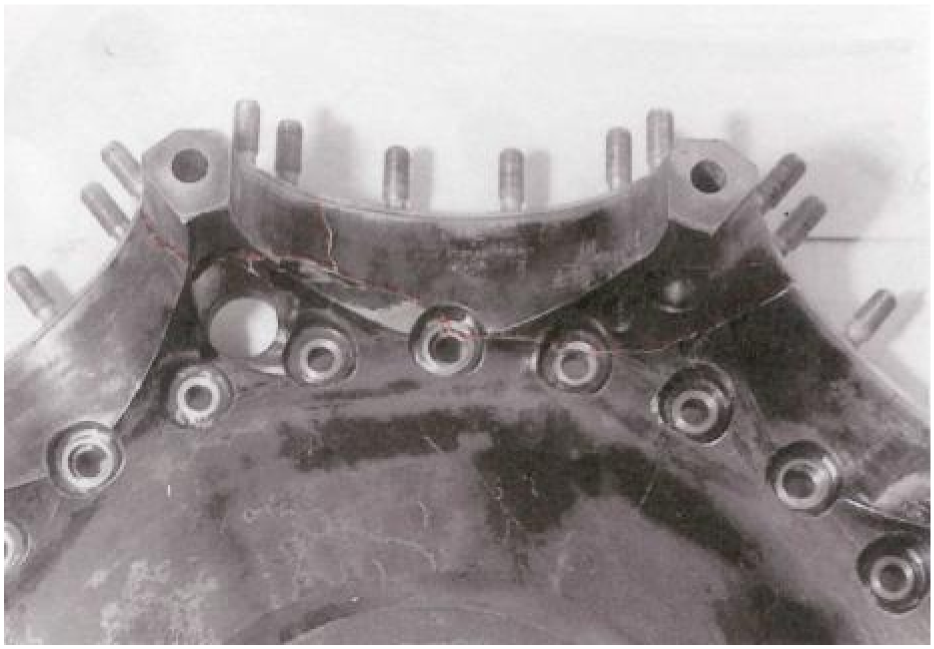

Fig. 10. Crack in the rear part of crankcase

The investigations into damages of the rear parts of the crankcases comprised the following issues:

- X-ray radiography,
- macro- and microscopic investigations,
- determination of the strength characteristics,
- fractography,
- chemical composition analysis.

The investigations conducted showed that the cracks that appeared in the crankcases were of the fatigue nature. The cracks initiated in the area of ends of threaded pins which were screwed into the crankcase.

The 3D FEM model (Fig. 11) of the rear part of crankcase was generated for the purposes of stress analysis aiming at the determination of stress concentration areas. The load spectra were determined for the rated power and take-off power, respectively.

Fig. 12 shows the distribution of reduced stress (the Huber hypothesis). It is clearly visible that the stress concentration occurs in the area of 27 holes ϕ 11 for bolts joining the crankcase with the compressor.

As a result of the analysis conducted the decision was made to introduce some changes into the design. Now, due to economic reasons at the current level of production it is impossible to change the crankcase shape. However, the following improvements can be made:

- raising the quality of threads in holes and threaded pins;

- making the blind hole depth more shallow;
- replacing the material used with the one revealing higher strength;
- laser shot peening.

After the aforementioned changes will have been introduced the fatigue tests will be made in co-operation with Warsaw University of Technology.

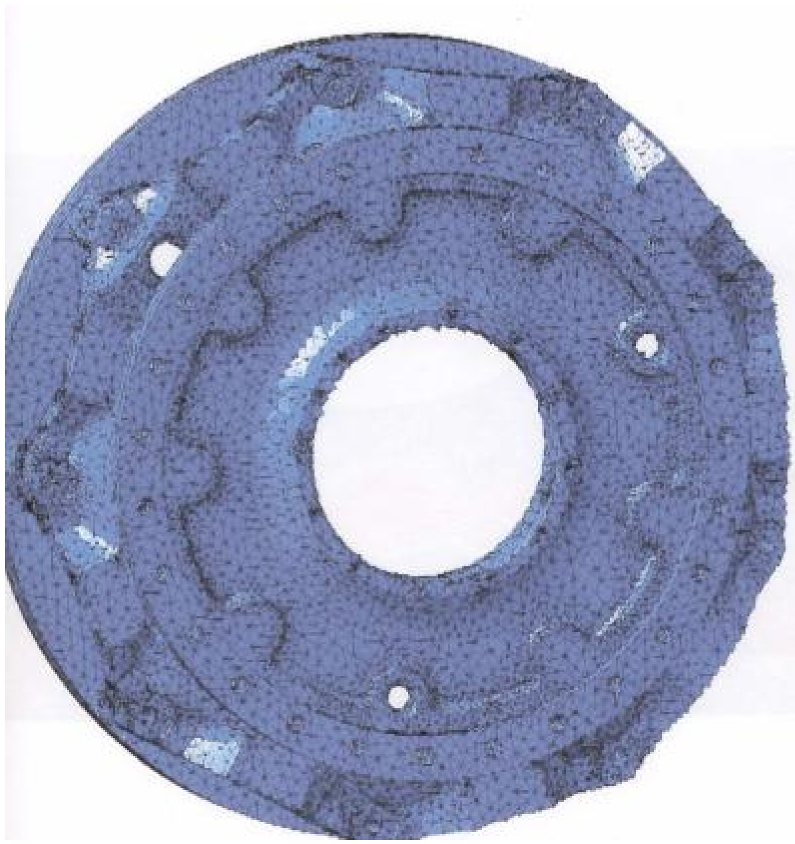

Fig. 11. 3D model of the rear part of crankcase

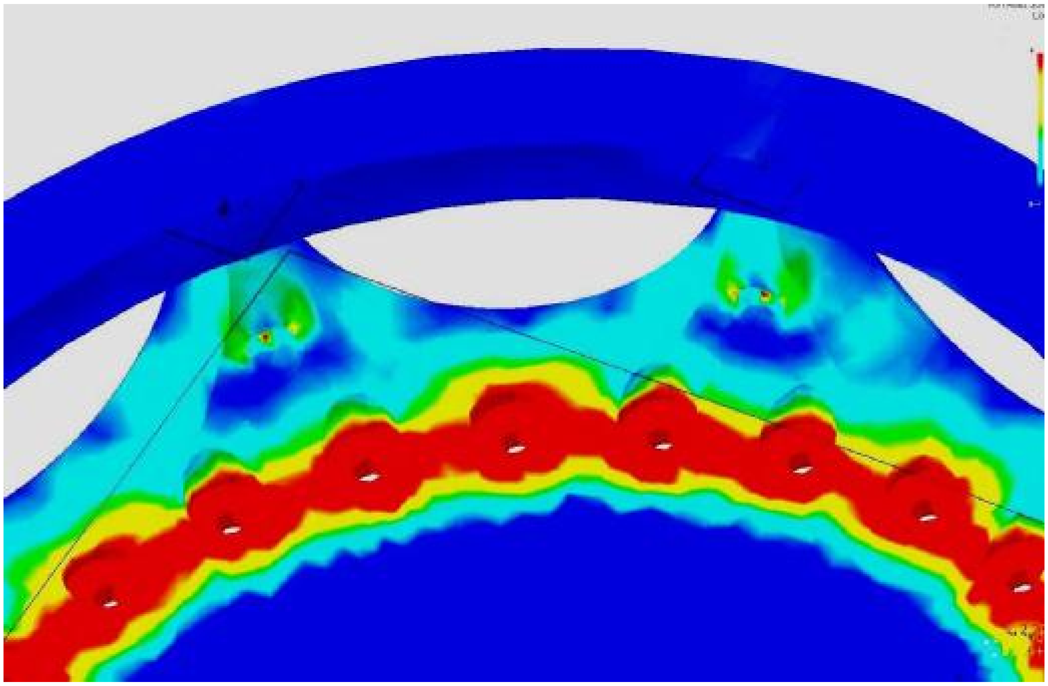

Fig. 12. The distribution of reduced stress (Huber hypothesis)
(maximum values in red)

Fan-cowl A318 Hinge Fitting and Latch Housing Static and Fatigue Tests
(Sebastian Szałkowski – ILOT)

Static and fatigue tests of hinge fitting and latch housing of the A318 fan-cowl are being carried out at the Institute of Aviation to order of CASA EADS in Madrid.

Each test specimen consists of hinge fitting or latch housing joined to the representative panel (two panels in the case of latch housing specimen) of the surrounding area, including beams and stiffeners. Two similar specimens of each element were manufactured, one for static tests and the other for fatigue tests. The specimens were made mainly from steel and aluminum alloys.

The Institute of Aviation designed and built the test set-up and installed the hydraulic loading system, the control system and the measurement and the data acquisition system. The entire test set-up for each specimen consists of the frame which restrains a specimen and one-channel load introduction system. Fig. 13. shows the test set-up with the hinge fitting specimen (one of the configurations) and Fig. 14. shows the test set-up with the latch housing specimen. 137 channels for the strain gauges and 3 displacement transducers for both specimens were necessary for measurement of the behavior of specimen structures during the static tests as well as fatigue tests.

The static tests were performed up to the limit load and then to failure of the specimens. Both specimens successfully withstood the required limit and ultimate loads.

The fatigue tests consist of three phases: fatigue, damage tolerance and residual strength. Until May 2005, 64 000 fatigue cycles (FC) which correspond to one service life, were successfully accomplished. The inspection program includes visual inspections every 8 000 FC and non-destructive inspections (high frequency eddy current method) every 32 000 FC.

Both static and fatigue test are carried out at room temperature and without specimen conditioning.

Figure 13. Test set-up with the hinge fitting specimen.

Figure 14. Test set-up with the latch housing specimen.

INVESTIGATIONS CONDUCTED BY RTD AND ACADEMIC CENTERS

Methods for Local and Microlocal Analysis of Physical Phenomena Emerging in the Vicinity of Riveted Joints in Thin-Walled Aircraft Structures

(Jerzy Jachimowicz, Wiesław Szachnowski – ILOT)
(Project conducted in co-operation with WAT)

The work aims at the development of methods for analysis of the riveted joints in aircraft structures. The effect of fretting (frictional corrosion) has been chosen as one of the most interesting physical phenomena that emerge in the vicinity of a rivet and accelerate the fatigue processes. The investigations are being conducted in terms of the FEM analysis and modeling of the aircraft riveted joints as well as the experiments made on specimens of riveted joints of a special design, in which the fretting phenomena occur. The specimens were made mainly of light alloy (of D16 grade, Russ, spec.) plated sheets and the rivets were made of steel (St3 grade, Polish spec.). The specimens and fatigue-testing stand are shown in Fig.15 a) and b).

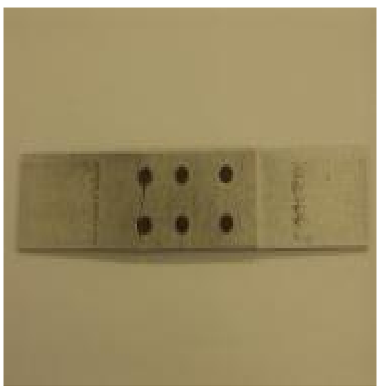

a)

b)

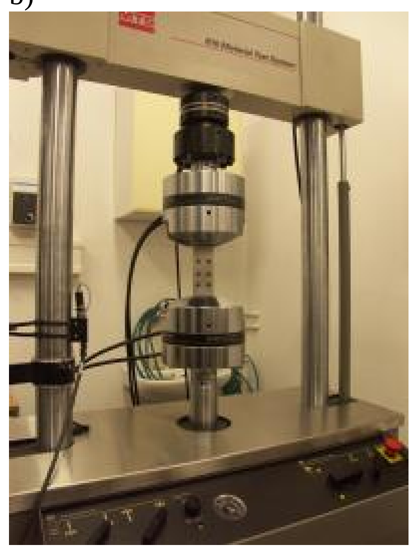

Fig.15.Specimen: a) overall view. b) the specimen at the testing stand

Up till now, the specimens have been examined using the NDT methods; such as, brittle coatings, magnetic, luminescent, wedge light. A set of strain gauge bridges was also installed. The X-ray diffraction measurements and metallographic investigation are being conducted as well.

We do hope that as a result of these investigations we will be able to understand better the mechanism of fretting initiation in the riveted joints.

A Measurement Program for the SU-22M4 Operational Loads
(Mirosław Nowakowski, Jarosław Krzonkalla – ITWL)

A measurement program of operational loads was carried out on the SU-22M4 aircraft. The flight parameters were recorded as well as the outputs of 72 strain gauge bridges located on various elements of the structure.

Fig. 16. SU-22M4.

The program aimed at providing the data necessary for validation of numerical models of some selected elements of the structure and for analysis of their fatigue life.
The program was fulfilled using the KAM-500 measurement system. The calibration procedure was followed at the beginning of the test to allow for formulation of the relationships between the structural loads and strain gauge outputs. For verification purposes this program was fulfilled once again after the operational load measurements had ended.
The measurement program comprised all the tasks that are executed during the pilot training program. The results obtained allow for the determination of operational load spectra and validation of numerical models.

Analysis of Low Cycle Fatigue Problems in Constructional Steel
(Sylwester Kłysz – ITWL)

In view of assessment of the fatigue life of constructional elements at the design stage, in operation as well as in analysis of possibilities of making it longer, it is very important to know fatigue characteristics of constructional materials; e.g., the fatigue life under low cycle fatigue conditions. The study presents a survey of basic issues of the problem of low cycle fatigue of metals together with the methods for presentation of the test results. The Authors focused their attention on the relationships between the fatigue life and strain range applied in tests, material strength properties, size of the hysteresis loop as well as the load sequence.

Macroscopic changes occurring in metal when subject to cyclic loads are presented in terms of a cyclic hysteresis loop, for this reason the loop representation and the cyclic strain curve are crucial in low cycle fatigue analysis. The algorithms are presented for calculation of the area of cyclic hysteresis loop that has been registered in low cycle fatigue tests. The sum of hysteresis loop areas is a critical parameter in analysis of fatigue life of the tested material. It seems reasonable to accept the assumption that the size of hysteresis loops represents the number of cycles equal to the half-life value. Taking the hysteresis loop area as a factor in analysis of the 2nd or 3rd load cycle may result in reaching accuracy of about 30-50% in fatigue life assessment, despite some exceptions, which should be taken into account

An important fact emerging from the presented relationships between the sum of hysteresis loop areas and the number of cycles to failure, is that the results obtained reveal the sensitivity hundred times higher than those resulting from the Manson-Coffin diagrams.

Selected Methods for Fatigue Testing and Analysis of Constructional Element Durability

(Sylwester Kłysz -ITWL)

The study presents a survey of selected fatigue test methods and strength analyses of construction elements. The statistical nature of fatigue and crack growth characteristics require long-term investigations and a significant research effort to prepare their theoretical study before its implementation. The general characteristics of fatigue strength problems, with a focus on the procedure algorithms employed during strength assessment for the initiation of fatigue cracks and propagation life are given. The fatigue life estimated according to those algorithms can be burdened with a discrepancy in relation to a real service life.

General relationships of the rate of fatigue crack growth, a new approach to the crack growth description (a multi-parameter equation and a model of a constant probability of crack growth) and the numerical procedure of estimation of the values of the propagation equation parameters, on the basis of experimental results (N_i, a_i) – the number of crack cycles and crack length, have been discussed. The results of fatigue crack propagation tests and specimen selection analyses were presented. The results of tests carried out on two different types of specimens (CCT and SEN) were compared.

An example of fatigue durability estimation and a crack propagation in the main wing beam near the bolts connecting it to the aircraft fuselage have been presented taking into account the load spectra registered during operation. In determination of the load spectrum of the wing and fuselage connection, two sets of information were used, coming from:

A) operation, based on 4443 flights, lasting 117646 minutes, made in various units on training/fighter jets. The set of information relates to training and combat flight structures with the duration provided for their particular types (tasks, number and ceiling);

B) measurements of fuselage and wing loads for typical flight stages, made in 6 flights. A different pilot, according to the same program and attempting to acquire maximum loads, performed each flight.

The load spectra for the 6 pilots, respectively, allowed for the analysis of the impact of differences between piloting methods on aviation structure durability. They indicate the particular meaning of in-flight measurements and flight-by-flight analysis of durability degradation of the structure.

Strength and Fatigue Tests of Polymethyl methacrylate (PMMA)
(Sylwester Kłysz – ITWL)

Most of recently used aircraft have cockpit canopies made of polymethyl methacrylate. Some important properties of the PMMA include: high hardness and stiffness, good environmental resistance and thermal strain, transparency, high surface polish, scratch resistance. At the same time, however, it is crack-sensitive under stress and flammable. Surface scratch and chipping are damages that most often occur in service. To prepare a cockpit canopy repair methodology it is necessary to know basic strength and fatigue material characteristics.

Flat specimens of rectangular cross-section cut out from the cockpit canopy material, in two perpendicular directions, were tested (according to GOST 11262-80 and GOST 9550-81 standards). The strength tests were aimed at determining the stress-strain curve parameters (the Young modulus, yield stress, endurance stress, elongation) within the (–40 ÷ 60) ^{o}C temperature range. Changes thereof in subsequent tension tests and the effect of hysteresis of mechanical properties were analyzed and statistical analysis of results - conducted. Thermal expansion of the PMMA was tested.

Fatigue tests of compact tension specimens, were made to determine the crack propagation rate vs. the stress intensity factor range under both the constant amplitude and controlled stress intensity factor range conditions. For $\bullet\ K < 1\,MPa\sqrt{m}$, the crack propagation rate is above 10^{-4} mm/cycle. The Paris equation coefficients for this condition are: $C = 10^{-1} \div 10^{-2}$, $m = 6.2 \div 7.5$.

Fatigue Investigations of Aluminium Alloys in the Military University of Technology
(Dorota Kocańda – WAT)

Fatigue investigations for two aerospace aluminium alloys – 2024-T3 alclad sheet and Russian alloy D16 alclad and additionally anodized sheet under different types of VA loadings were conducted. The main goals of this research were either the exploration of the load sequence effect on fatigue crack growth in short and long crack ranges for the CCT specimens (100 x 400 x 3 mm) cut along (LT) and perpendicular (TL) to the sheet rolling direction or the capability of the load-time history reconstruction on the basis of macro and microfracture analysis. The programmed loadings like as: Low-High-Low (L-H-L), Flight-after-Flight (F-a-F), zero-to-tension (R = 0.1) VA loadings with multiple low overloads (k_{ovl} = 1.25) imposed on the baseline cycles and CA tension (R = 0.1) and CA bending (R = 0.1) (for any comparison study) corresponded to flight simulation spectrums of a lower skin aircraft wing structure.

The experimental results obtained have proved that in the range of long cracks (over 3 - 4 mm crack length) the fatigue crack growth rate was about 1,5 times higher in TL type specimens than in LT ones in each case of VA loadings. In CA both cyclic tension and bending no differences were found. In the range of short fatigue cracks were observed great discrepancies of their growth rates, resulting from difficulties in recording of the early crack extension in alclad thin surface layer in the case of 2024-T3 alloy. In D16 aluminium alloy sheet this early crack extension runs firstly under anodizing thin surface layer and then on the specimen surface and in the alclad layer. In the aluminium alloys is observed big influence of the load sequence effect, particularly the succession and amount of overloads appeared in the load sequence on the crack growth rate and fatigue life time. Similar L-H-L and F-a-F load sequences with respect to the range of the stresses but differing both from the order and number of overloads in the load program provide different fatigue lives of a component (Fig. 17). Considering the life time of component the most favourable VA load program turned out the L-H-L one. The CA loading leads to the lowest life time. Generally, more complex VA load programs containing the overloads impose more severe limitation on the reconstruction of the load-time history on the basis of fatigue striation systems formed on the fracture surface. Microfracture analysis done by means of the SEM and TEM microscopes (Fig. 18) proved that under the L-H-L program the period of crack propagation covers less than 10% of the load program duration whereas in the case of F-a-F program 26% of total time is devoted to the crack propagation. In Fig. 19 (a) and (b) crack length was estimated on the basis of fatigue striations spacing formed on the fracture surface. As can be seen most part of these load program durations is spent on crack arrest or crack growth at a very low rate. This crack behaviour results from the plastically induced crack closure effect as well as the crack penetration through the plastic zones associated with the overloads.

For prediction of the crack growth under VA loading and estimation the fatigue life of a component were developed both deterministic and probabilistic approaches. The crack retardation model is based on the Wheeler model.

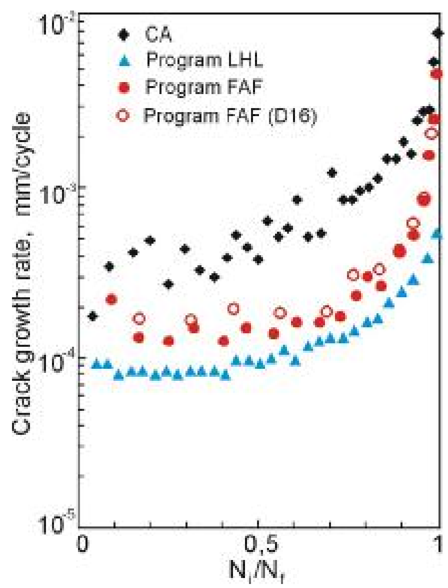

Fig. 17. Influence of the applied loadings on the fatigue crack growth rates in 2024-T3 aluminium alloy sheet against cycle ratio Ni/Nf

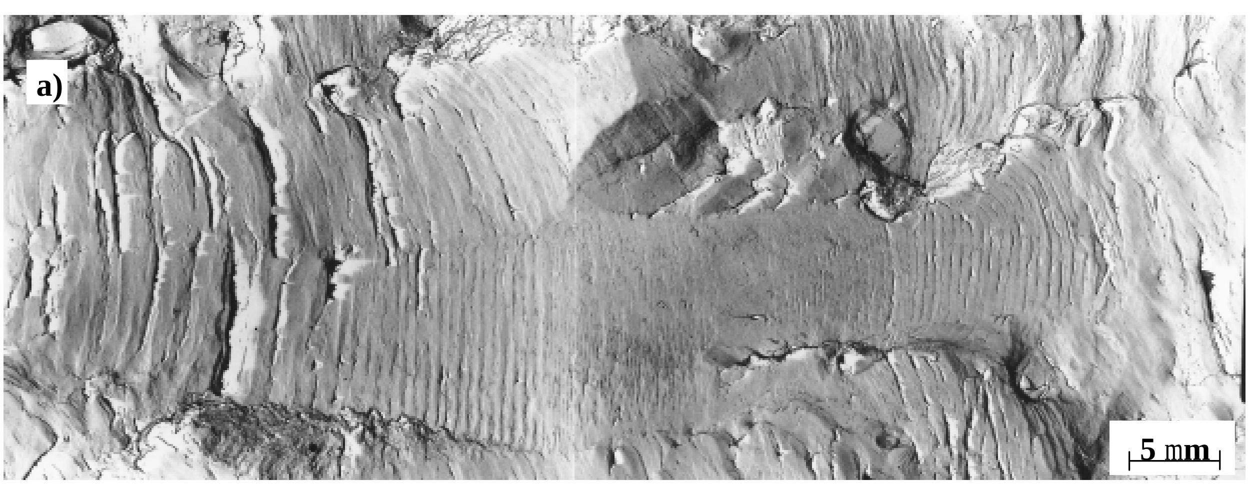

Fig. 18. TEM micrographs illustrating the fatigue striation systems on the fracture surface of 2024-T3 alloy under the LHL load program at a distance of 5-8 mm (a) and 8-11 mm (b) from the notch (CCT sample).

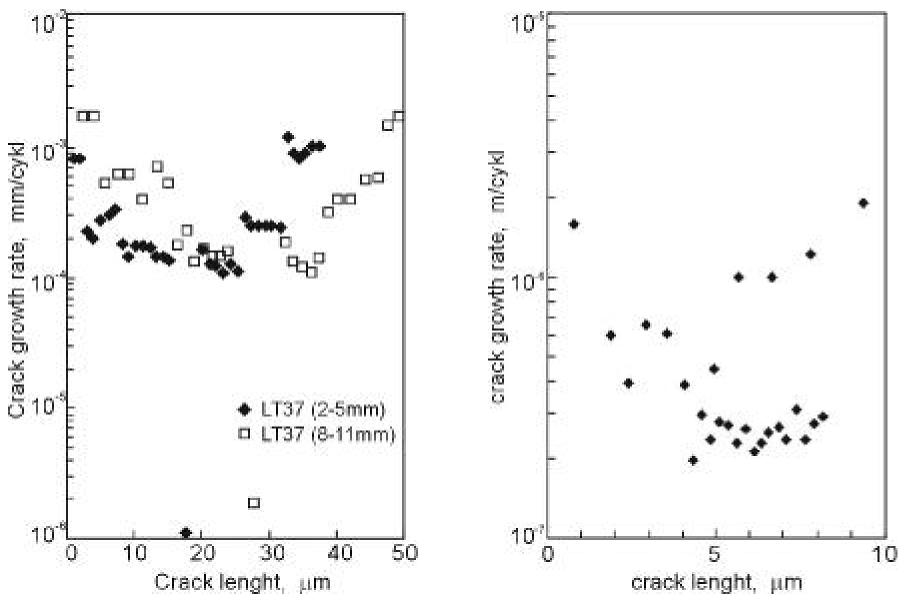

Fig. 19. Variation of fatigue crack growth rates on a microscopic scale within one load sequence of the LHL load program (a) and FAF program (b) against crack length.

FATIGUE LOADS AS AN INVERSE PROBLEM OF THE HELICOPTER TAIL BEAM STRUCTURAL DYNAMICS

Janusz DYMITRUK[1], Ludomir M. LAUDAŃSKI[2]

Key words: helicopter structural dynamics, fatigue loads, inverse problem of dynamics

Abstract: The paper presents a brief report related to the experimental research done under substantial financial support from the side KBN (National Scientific Research Council, Poland) in the Structural and Component Test Laboratory of the Aviation Institute in Warsaw, Poland. The tail beam of the 'Sokol' helicopter was under experimental investigation going to work out a method enabling to determine such external loads (assuming to impose them by three hydraulic actuators) which caused in the tail beam structure at five given cross sections a priori given loads being a combination of bending and twisting moments of the prescribed magnitude. These in turn were selected in test flights by a Polish helicopter factory research project managed prior to this investigation. It was earlier established that such elastic structure as a helicopter tail hardly enables to involve experimental fatigue loads due to a serious threat of a damage done before the fatigue life is assessed. Such a demand gradually led to the precise formulation of the problem which afterwards has been successfully solved fulfilling practically accepted accuracy requirements. The paper presents the main idea of the optimization procedure which became the main part of the research worked out in a due course and particularities of the numerical calculations belonging to the research documenting the efficiency of the proposed method.

1. GENERAL CONCEPT AND ITS EXPERIMENTAL IMPLEMENTATION

The main aim of the paper, following extended literature studies (quoted papers [1] – [12] reflect only few arbitrary chosen) has been oriented towards determining the experimental method enabling to find such external harmonic loads which applied in fixed a priori sections of the tail beam of a helicopter design will result in a priori given inner loads of the structure. Therefore, the work lead to work-out an algorithmic procedure which further would be used to complete a fatigue experiment of such a structure to determine its fatigue life under given environmental loads registered during the service of such a vehicle. Having in mind this fact all the details as how to manage the entire experimental tools and components – how to chose the control sections, how to chose the places and how to fix strain gauges as well as how to collect them into particular strain gauge measuring points regarding particular testing sections were managed. Those testing sections once have been statically scaled – became reliable sources to measure bending moments in both - vertical and horizontal planes – and also regarding the twisting moment. Some details are given in Fig.1. Bending moments were defined in sections D, B and G1, while twisting moments in sections F and E. Those 5 sections were controlled by the 8 strain gauges. Therefore, harmonic vibrations were registered by 6 amplitudes of the bending moments and 2 amplitudes of the twisting moments. In Fig.2, 3 and 4 have been presented the target moments in all prescribed sections of the tail beam under investigation. The previous experience in this field recommended as technically possible to manage three external forces S1, S2, and S3 - applied in the prescribed below way (see also Fig.5 and Fig.6):

(1) S1 - situated aslant in the plane of the intermediate transmission – applied in a view of two perpendicular components – situated horizontally and vertically;
(2) S2 - always acting horizontally to produce twisting moments;
(3) S3 - also acting aslant at the rear transmission junction center – applied in a view of two perpendicular components – situated horizontally and vertically.

[1] Aviation Institute, Warsaw
[2] Rzeszow University of Technology, Poland

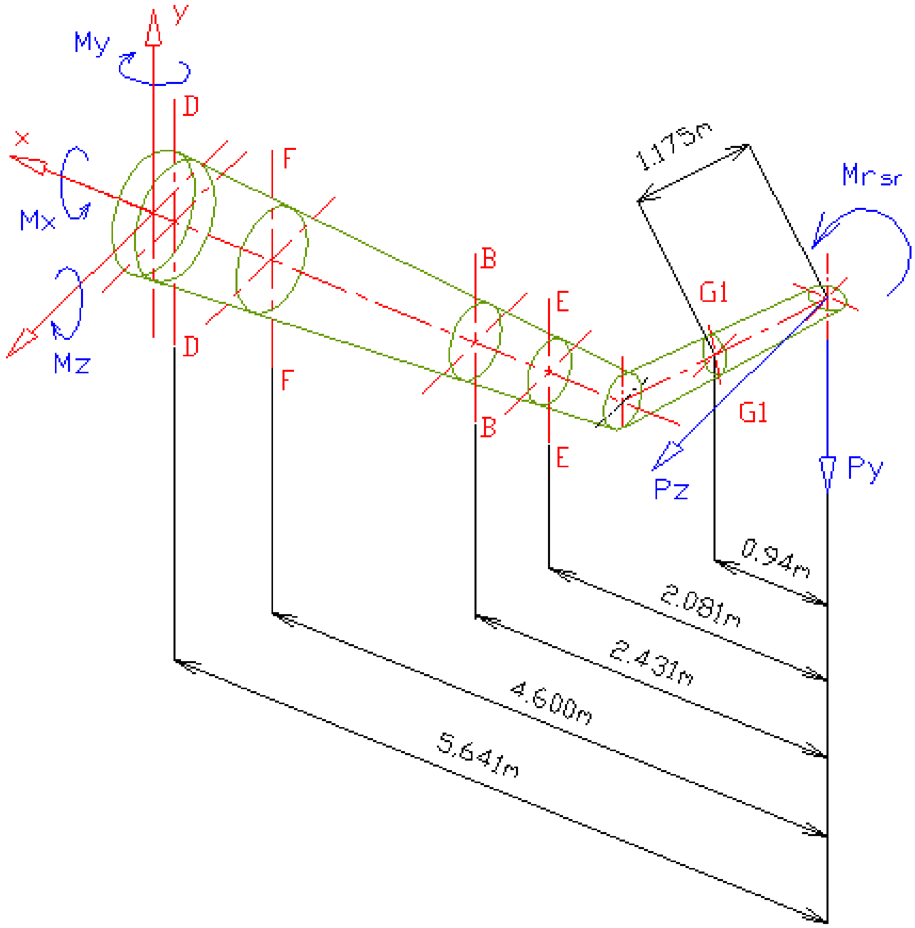

Fig.1. Tail beam, its geometry, and symbolic character of the simulated loads

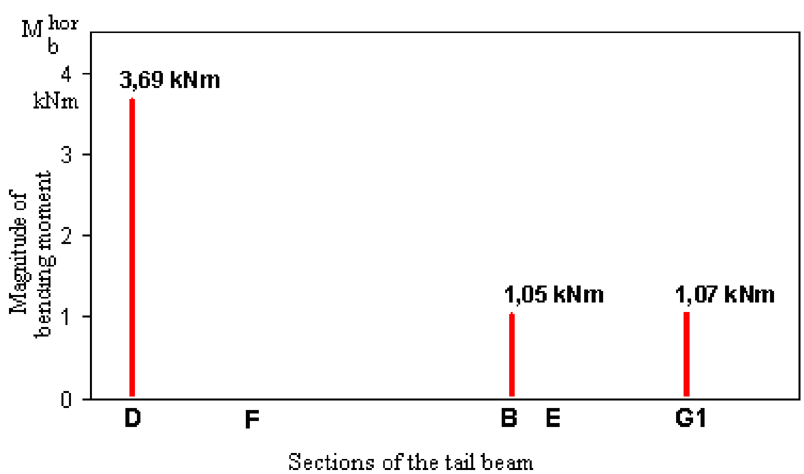

Fig.2. Target bending moment acting in the horizontal plane along the tail beam

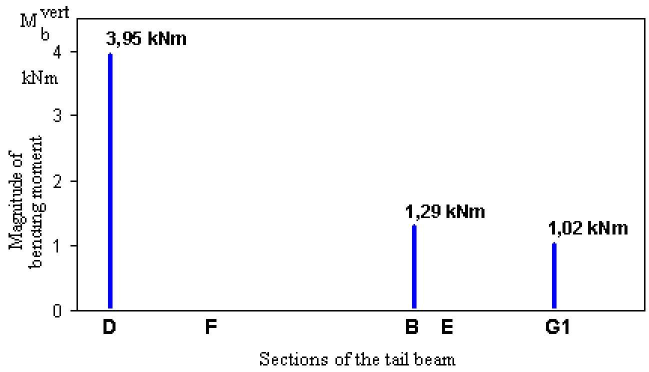

Fig.3. Target bending moment acting in the vertical plane along the tail beam

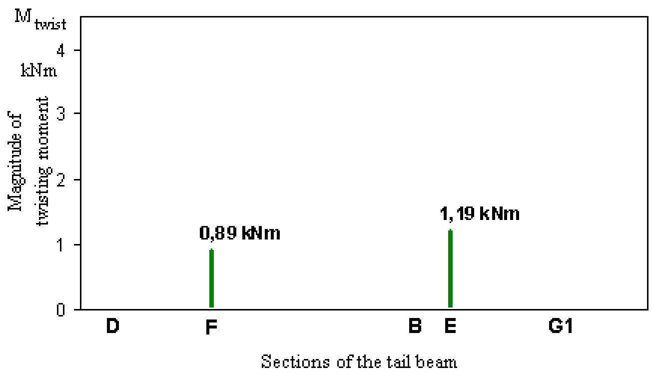

Fig.4. Target twisting moment acting along the tail beam

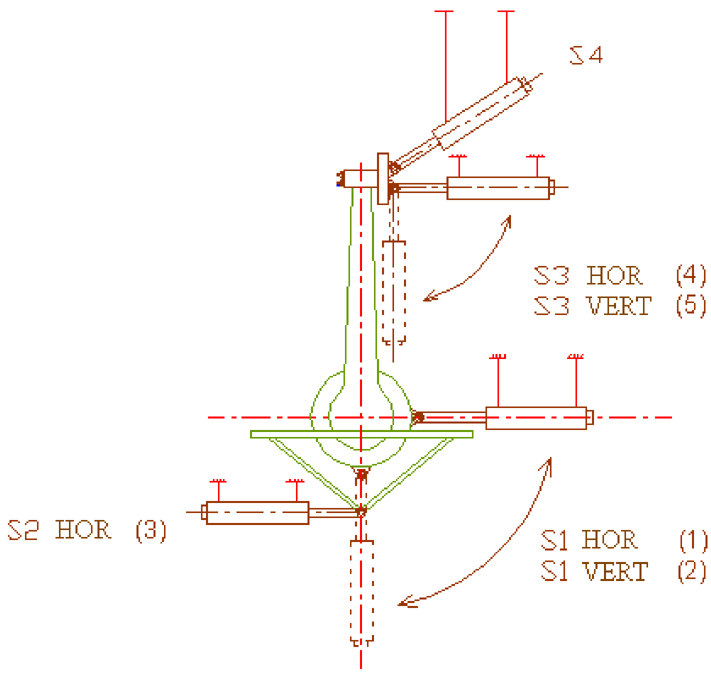

Fig.5. Positioning of the hydraulic actuators used in the experiment – rear view

Fig.6. Rear view from the right side of the experimental stand showing actuators

Loads prescribed in Fig.2-4 – were reproduced by using frequency upper band i.e. frequencies between 18 and 22 Hz. While S4 actuator has been installed for the purposes of the lower frequency range i.e. frequencies lying between 6 and 8 Hz. Numbers shown in Fig.5 describe the succession used to supply power to the actuators – and also the succession used in evaluation of the measured quantities. To determine all the values of the transfer functions the actuator had to manage the stable vibrations with the step 0.1 Hz among successive frequencies preserving the level of the appropriate responses of order a dozen or a few dozens of the values desired by the computer optimization program. The particular transfer function was defined as a response of a particular strain gage regarding the unit exciting force – therefore having in mind 8 measuring quantities (see Fig.2, Fig.3 and Fig.4) and 5 possibilities to actuate vibrations (see Fig.5) – it gives 40 transfer functions – each one has to be fixed by 70 frequencies. All of this gives us the right impression regarding the complexity and the entire experiment volume.

2. THE METHOD OF OPTIMISATION – THE IDEA OF THE PROCEDURE

Identification stage of the dynamic properties of the tail beam under consideration can be understood as a set of forty Transfer Functions (specified above). To give the Reader a chance to inspect them it would be necessary to present those functions altogether (showing their modulus and phase angle) in the full range of the frequencies. This stage has been provided only within [11] which is going to be published by the Aviation Institute – Warsaw, Poland soon. So the enquiring Reader is advised to make use of this publication. Here we show only a little extract of this broad picture – as successive – Fig.6 and Fig.7.

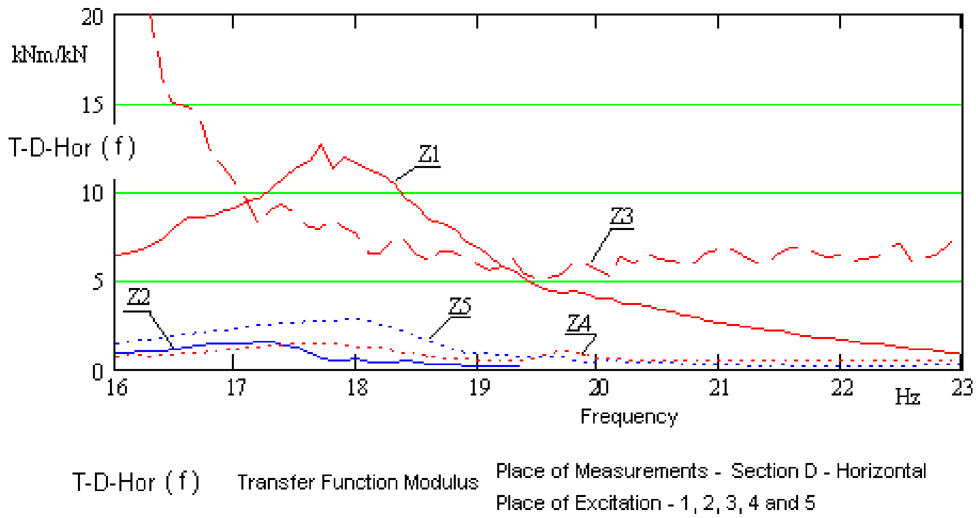

Fig.6. Transfer Function Modulus – Horizontal Bending Moment at Section D as a Result of Excitation – Accordingly by S1-HOR, S1-VERT, S2-HOR, S3-HOR and S3-VERT

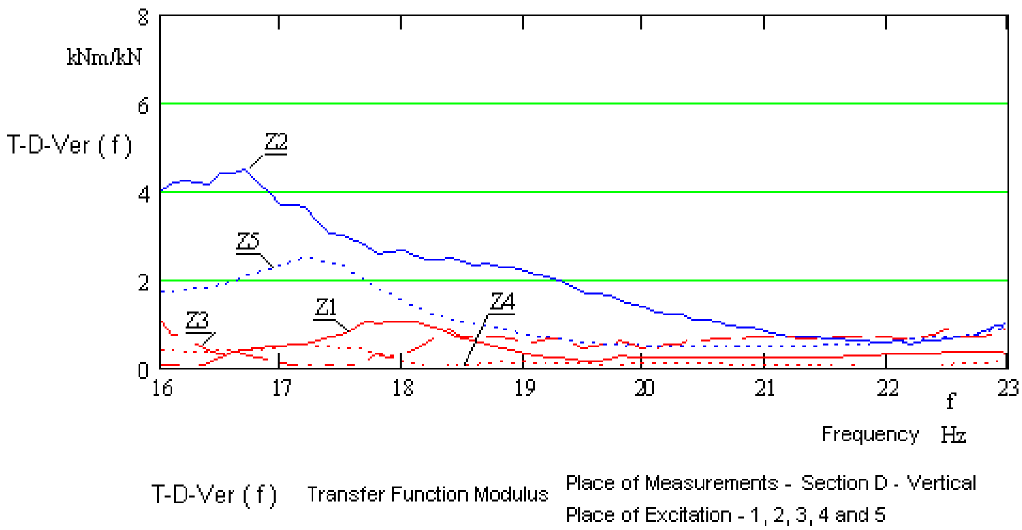

Fig.7. Transfer Function Modulus – Vertical Bending Moment at Section D as a Result of Excitation – Accordingly by S1-HOR, S1-VERT, S2-HOR, S3-HOR and S3-VERT

Instead of the detailed comments it is proposed to note two different vertical scales in Fig.6 and Fig.7, then - the high sensitivity of the both bending moment components within the range of the lowest frequencies indicating resonance conditions, as well as essentially different levels of sensitivity regarding the particular exciting forces for all the ten cases shown in these figures. We skipped the other side of the picture – i.e. the phase between the source actuators and the recipients, simply in order to save the length of the paper.

Now we shall brief some topics regarding the numerical algorithm to evaluate experimental data. The eight target values of the moments acting in the sections indicated in Fig.1 and Fig.2 have been denoted by:

$$U^j \quad \text{where} \quad j = 1, \ldots, M \tag{1}$$

Initially – so to speak – the outcome *Z* of the excitation caused by the actuator denoted by '*i*' registered by the ***j-th*** strain gauge has been denoted as:

$$Z_i^j \quad \text{where} \quad i = 1, \ldots, N \tag{2}$$

Taking into account that all the five actuators will work simultaneously their resulting effect will be seen as a weighted superposition, therefore for the ***j-th*** strain gauge we expect the result in the form:

$$\sum_{i=1}^{N} A_i \cdot Z_i^j = R^j \tag{3}$$

The simplest description of the proposed idea of the optimization takes the form:

$$f(A_1, A_2, \ldots, A_N) = \sum_{j=1}^{M} \left(\frac{R^j - U^j}{U^j} \right)^2 \Rightarrow \min \tag{4}$$

The formal conditions leading to satisfy requirements expressed by (4) have the form:

$$\frac{\partial f}{\partial A_i} = 0 \tag{5}$$

We skip the particularities of this well known formal procedure stating that in this way all the desired coefficients A_i can be determined. This is the main idea of the procedure which in its real implementation requires to operate with the complex quantities, that is each Z_i^j has in fact the form:

$$Z_i^j = \mathrm{Re}\left(Z_i^j\right) + i\,\mathrm{Im}\left(Z_i^j\right) \tag{6}$$

Therefore, the final set of the algebraic equations leading to determine all the weighting coefficients A_i takes accordingly more developed fashion and in order to avoid the redundant technical matters we do not import here such detailed results from the pages [11]. The final outcome of this formal procedure has been presented in a more readable pictorial form in Fig.8.

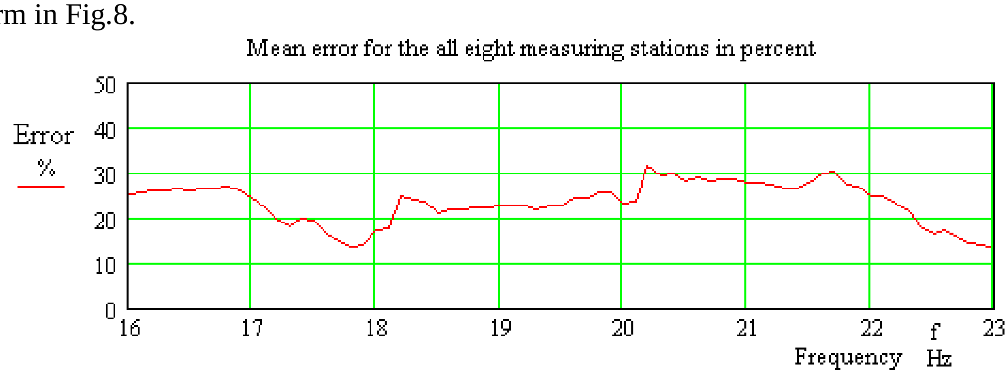

Fig.8. Average percent error for the all eight simulated results

Regarding numerical values of the weight coefficients their two typical outcomes are shown in Fig.9. The requirements indicated by the formula (4) and (5) – in a natural way lead to the iterative procedure. In the first loop all coefficients A_i are assumed to be unit. Then – solving the system of five algebraic equations fulfilling condition (5) – gives the next approximation. We leave the details of the particularities regarding them.

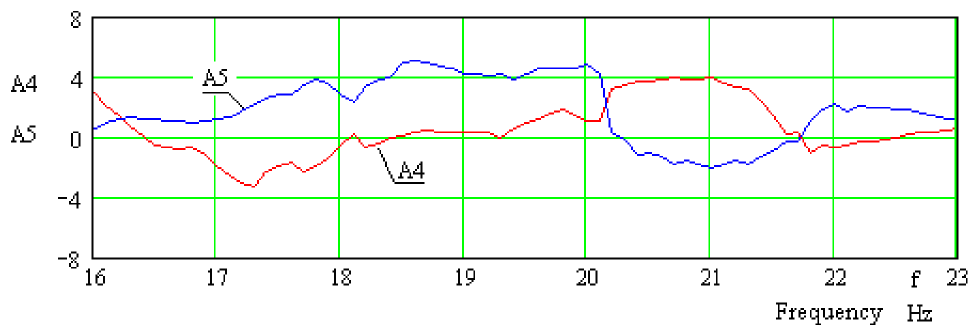

Fig.9. Coefficients A_i for two typical cases - obtained in four iterations

With the obtained weight coefficients there is a variety about 70 cases to choose while simulating demanded load for any particular case of simulation. In Fig.10 are shown results of two simulations (choosing frequency 17.3 Hz) – both regarding bending moments acting in horizontal plane – accordingly in section *D* and section *G1* (see Fig.2). The dropped line indicates target value (its true value is to be read in Fig.2), while continuous line shows how the five contributors – denoting actuators shown in Fig.5 (preserving also the succession shown there) – are composing the simulated one. The gap between both vectors can serve as a discrepancy measure – i.e. documents pictorially the final error of the simulated value.

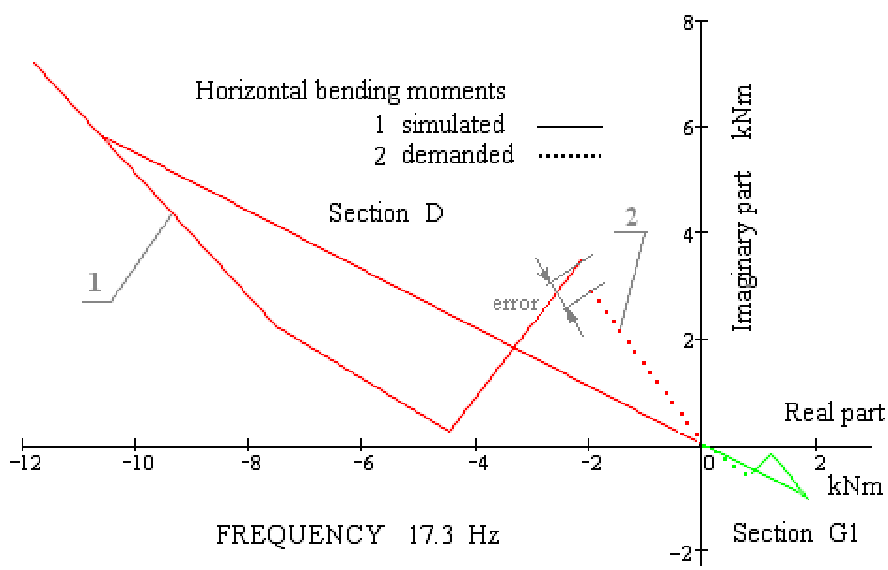

Fig.10. The final simulation as contributed by five actuators – showing the error

3. THE PROBLEM OF THE THREE ACTUATORS

As it is seen from Fig.5 – and also – from the above mentioned theoretical considerations – up to this point we proceeded engaging five actuators. It was our firm supposition that applying actuators either horizontally or vertically we are in the right position to proceed with the detailed identification of dynamic properties of the tail beam structure under consideration – in a view of the appropriate transfer functions. On the other hand – having in mind the future fatigue testing to determine the fatigue life of this structure – especially some features of the Laboratory accessed in the Institute of Aviation in Warsaw where this research has been proceeding – it has been decided for achieving this goal to use only three actuators. It means that regarding the junction of the final transmission (shown in the upper part of Fig.5) – instead of two actuators – denoted as S3 HOR and S3 VERT – should be applied only a single one – directed diagonally. The similar situation occurs with the junction of the intermediate transmission (shown in the lower part of Fig.5) – regarding actuators denoted as S1 HOR and S1 VERT. The point is: which direction to follow (for both actuators) has to be preserved and how to determine this direction? It must be immediately stated that the obvious solution to place such a single actuator preserving the Cartesian components resolution – determined by the values of forces applied horizontally and vertically – the experiment rejects entirely. It has been found with certainty that the parallelogram rule does not work. For the linear systems the rule of superposition works so well that in theoretical approaches it becomes one of the two axioms to define a linear system (the other one becomes the linear proportionality). Therefore, the lack of the superposition becomes a symptom of non-linearity and in such a case one has to determine how to proceed in order to replace the effect of applying two actuators acting in perpendicular directions by a single one acting diagonally. This problem has been so far solved tentatively by resorting to some procedure described symbolically by the verbal sentence expressed as follows:

„ a circle of the unit excitation $\Leftrightarrow$ an ellipse of the response ”

Therefore, we have to commence with the geometrical features of the procedure and we propose first to examine Fig.11.

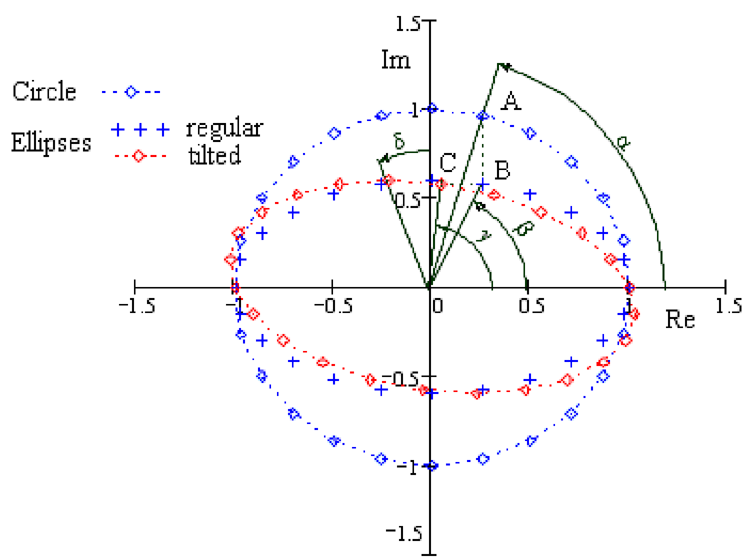

Fig.11. Geometric relation between a unit circle and two ellipses

In Fig.11 the simplest geometrical meaning shows the angle d which indicates the angular position of the so-called 'tilted' ellipse. The other three angles are referring to the second order procedure postulated to admit the non-linear character of the structure under consideration. This geometrical aspect of the relations among three curves draw in Fig.11 reflects projections of a single point – denoted by 'A' on a unit circle, by 'B' on the regular ellipse, and by 'C' – on the second ellipse.

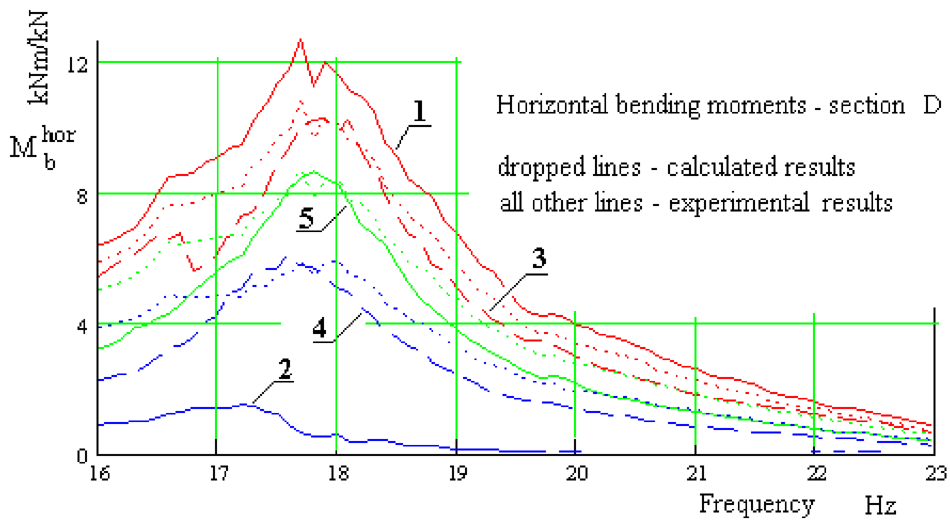

Fig.12. Relation between experimental and calculated results

The closing picture is shown as Fig.12. All experimental results shown in this figure have been measured at section D and obtained by applying the actuators described below applied at the junction of the intermediate transmission (shown at the bottom part of Fig.5. The result indicated at the top of the figure – denoted by '1' has been obtained while the structure has been excited by the actuator S1 HOR. The lowest line – denoted in Fig.12 as '2' – was the response of the structure to the actuator S1 VER. One can see from the comparison the sensitivity of the examined structure regarding the direction of the actuator. To get results indicated by '3' – the actuator S1 has been shaking the structure at a special joint located in a way which allowed to achieve direction of the exciting force acting under angle 30 degrees relative to the horizontal direction. Similarly – to get the results shown as '4' – the actuator S1 has been applied in the diagonal direction – tilted regarding the vertical direction by 30 degrees. And finally the results indicated as '4' – correspond to the direction 45 degrees. We show here only modules of the measured quantity. Although the measurement regarding the phase was done simultaneously. These results in similar arrangement were conducted for the all possible combination between eight measuring point and indicated four combinations of the actuators acting at the junction of the final and the intermediate transmissions. The comparison between predicted and measured results were always of the order which we see in Fig.12. The research – described in [11] in detail – although in Polish language – was completed by the thorough error study. The paper [11] contains almost one hundred extend pictorial representations of such a procedure.

REFERENCES

[1] W.Weibull: Fatigue Testing and Analysis of Results. Pergamon Press, Oxford 1961.

[2] K.Sobczyk, B.F.Spencer, Jr.: Random Fatigue. *From Data to Theory.* Academic Press, Boston 1992.

[3] L.M.Laudański: Computational Probability for Aeronautical Engineering. Wydawnictwa Instytutu Lotnictwa, Warszawa 2002.

[4] R.E.Little, E.H.Jebe: Statistical Design of Fatigue Experiments. Applied Science, London 1975.

[5] Fatigue in Aircraft Structures. Edited by A.M.Freudenthal. Academic Press, New York 1956 . Paper of B.O.Lundberg: Fatigue Life of Airplane Structures – originally printed in JAS, v.22, No.6, pages: 349-402, 1955.

[6] O.Buxbaum: Betriebsfestigkeit. *Sichere und wirtschaftliche Bemessung schwingruchgefährdeter Bauteile.* Stahl - Eissen 1992.

[7] Julius S. Bendat: Principles and Applications of Random Noise Theory. John Wiley & Sons, 1971.

[8] Julius S. Bendat, Allan G. Piersol : Random Data: Analysis and Measurement Procedures. John Wiley & Sons, 1971.

[9] J. P. Den Hartog: Mechanical Vibrations. John Wiley & Sons, 1971.

[10] Tadeusz Kaczorek : The Control Theory (in Polish). PWN, Warszawa 1977.

[11] John R. Taylor : An Introduction to Error Analysis. *The Study of Uncertainties in Physical Measurements*. University Science Books, 1982.

[12] Wanda Szemplińska, Rościsław Aleksandrowicz: Ground Resonance Testing of Sailplanes, Proceeding of the 7th OSTIV Congress, Leszno, Poland, June 1958.